6.3.2 Examples of commonly-studied shear flows

Linear shear flows

As seen in the previous section, linear shear flows of the kind $\boldsymbol{u} = z\boldsymbol{e}_x$ are not expected to have any growing modes. Let's see this more directly by solving Rayleigh's instability equation subject to the boundary conditions $\hat{w} = 0$ at $z = -1$ and $z = 1$. Note how the velocity amplitude and domain height are now both non-dimensional. The equation simply becomes:

$$(z - c)\left(\frac{d^2\hat{w}}{dz^2} - k_x^2\hat{w}\right) = 0 \tag{6.1}$$

There are several possibilities:

- If c is real, and not in the interval $[-1, 1]$, then this can be rewritten as

$$\frac{d^2\hat{w}}{dz^2} = k_x^2\hat{w} \tag{6.2}$$

  which has exponential solutions. However, these cannot be fitted to the homogeneous boundary conditions so this case is ruled out entirely.

- If c is complex, that is, $c = c_R + ic_I$ where $c_I \neq 0$, then (6.1) has a real and imaginary part, which are respectively:

$$\begin{aligned} (z - c_R)\left(\frac{d^2\hat{w}_R}{dz^2} - k_x^2\hat{w}_R\right) + c_I\left(\frac{d^2\hat{w}_I}{dz^2} - k_x^2\hat{w}_I\right) &= 0 \\ (z - c_R)\left(\frac{d^2\hat{w}_I}{dz^2} - k_x^2\hat{w}_I\right) - c_I\left(\frac{d^2\hat{w}_R}{dz^2} - k_x^2\hat{w}_R\right) &= 0 \end{aligned} \tag{6.3}$$

  where $\hat{w} = \hat{w}_R + i\hat{w}_I$. These can be combined to get (for instance)

$$\left[(z - c_R)^2 + c_I^2\right]\left(\frac{d^2\hat{w}_R}{dz^2} - k_x^2\hat{w}_R\right) = 0 \tag{6.4}$$

  and similarly for $\hat{w}_I$. Since c_I was by assumption non-zero, we end up again with equation (6.2) whose exponential solutions cannot be fitted to the boundary conditions. This has a very important implication: remembering that $\lambda = -ik_x c$, we can only get growing solutions if c_I is non-zero – but we just ruled this possibility out. Hence, as expected, we find that there are no linearly unstable modes in linear shear flows.

- Finally, if c is real and lies within the interval $[-1, 1]$, then for any selected value of c, (6.1) is singular at the point $\bar{u}(z_s) = z_s = c$, and the derivative must be discontinuous at z_s. Solutions can be found by solving (6.1) on both sides of z_s, and matching them to one another at that point requiring continuity of $\hat{w}$.

  Solving (6.1) for $z > z_s$, and applying $\hat{w} = 0$ at $z = 1$, we get

$$\hat{w} = w_+ \sinh(k_x(z - 1)) \tag{6.5}$$

Similarly for $z < z_s$:

$$\hat{w} = w_- \sinh(k_x(z+1)) \tag{6.6}$$

Matching the two at $z = c$, we have

$$w_+ \sinh(k_x(c-1)) = w_- \sinh(k_x(c+1)) \tag{6.7}$$

This can be rewritten as

$$w_+ = \frac{w_0}{\sinh(k_x(c-1))} \text{ and } w_- = \frac{w_0}{\sinh(k_x(c+1))} \tag{6.8}$$

where w_0 is the total mode amplitude, which remains arbitrary since this is a linear problem. So finally, for every value of c in the interval $[-1, 1]$, we get one eigenmode $\hat{w}(z)$ as:

$$\hat{w} = \frac{w_0}{\sinh(k_x(c-1))} \sinh(k_x(z-1)) \text{ for } c \leq z \leq 1$$
$$\hat{w} = \frac{w_0}{\sinh(k_x(c+1))} \sinh(k_x(z+1)) \text{ for } -1 \leq z \leq c \tag{6.9}$$

A particular mode for $k_x = 1$, for $c = -0.2$ is shown in Figure 6.1. Note how $\hat{w}$ is continuous but its derivative isn't. This implies, by the continuity equation, that the horizontal flow velocity u is discontinuous. Of course, this can only happen in the non-viscous case (viscosity would otherwise tend to smooth-out the discontinuity, thereby disallowing this kind of solution). See more in the next section on the effect of viscosity on linear shear flows.

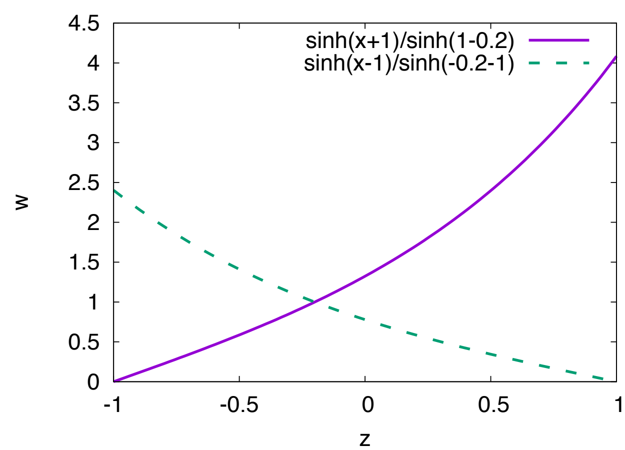

Figure 6.1: Vertical velocity profile for the neutral mode with $k_x = 1$, for $c = -0.2$

To summarize these results, we have seen that, as discussed in the previous section, a linear shear is linearly stable, but there is a continuum of neutral modes where the real part of c lies in between the minimum and the maximum of $\bar{u}(z)$. With $\lambda = -ik_x c$, the full solution for the vertical velocity is

$$w(x,z,t) = \Re\left(\hat{w}(z)e^{ik_x(x-ct)}\right) \tag{6.10}$$

where $\hat{w}$ is given in equation (6.9). The neutral modes thus discovered are a form of oscilation propagating in the x-direction at velocity c without change of form. Note that $\hat{w}$ has a kink in z, so by the continuity equation $\hat{u}(z) \propto d\hat{w}/dz$ must have a discontinuity. Any discontinuity in a real shear flow should be worrying, but here we can really attribute it to the fact that we ignored viscosity, and neutral modes with a little viscosity do in general merely becomes stable ones.

The Bickley jet

There are not many continuous profiles $\bar{u}(z)$ for which analytical solutions of Rayleigh instability equation exist. In general, solutions and their corresponding eigenvalues have to be computed numerically. In the following example, which studies the *Bickley jet*, some of the solutions can be found analytically, and some must be found numerically.

The Bickley jet is of the form

$$\bar{u}(z) = \mathrm{sech}^2(z)\boldsymbol{e}_x = \frac{1}{\cosh^2(z)}\boldsymbol{e}_x \tag{6.11}$$

and is shown in Figure 6.2.

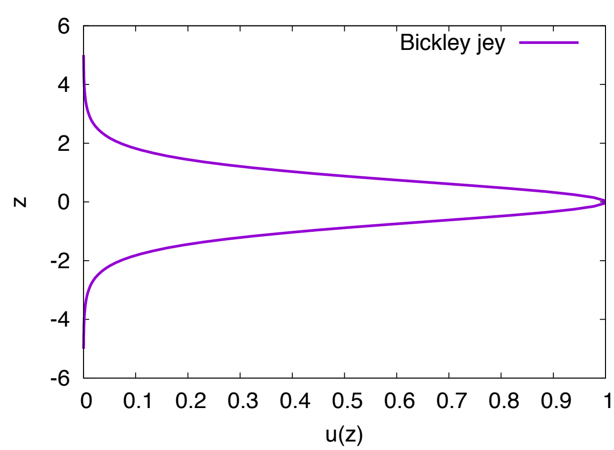

Figure 6.2: Bickley jet

The first and second derivatives are

$$\bar{u}'(z) = -2\tanh(z)\bar{u}(z)$$
$$\bar{u}''(z) = -2\tanh(z)\bar{u}'(z) - 2\text{sech}^2(z)\bar{u}(z) = 2(2-3\bar{u}(z))\bar{u}(z) \tag{6.12}$$

This has an inflection point at positions z_i such that $\bar{u}(z_i) = 2/3$ (which happens at two positions, one below 0 and one above 0). We therefore expect, for each value of k_x, at most 2 pairs of complex-conjugate modes. As it turns out, because of the symmetries of the jet, there are indeed 2 modes: one for which $\hat{w}$ is symmetric with respect to z (called the *sinuous mode*), and one for which $\hat{w}$ is antisymmetric with respect to z (called the *varicose mode*).

To find growing modes, one needs to solve Rayleigh's instability equation numerically. As before, we first isolate the real and imaginary parts of this equation, to get:

$$(\bar{u}(z) - c_R)\left(\frac{d^2\hat{w}_R}{dz^2} - k_x^2\hat{w}_R\right) + c_I\left(\frac{d^2\hat{w}_I}{dz^2} - k_x^2\hat{w}_I\right) - \hat{w}_R\bar{u}''(z) = 0$$
$$(\bar{u}(z) - c_R)\left(\frac{d^2\hat{w}_I}{dz^2} - k_x^2\hat{w}_I\right) - c_I\left(\frac{d^2\hat{w}_R}{dz^2} - k_x^2\hat{w}_R\right) - \hat{w}_I\bar{u}''(z) = 0 \tag{6.13}$$

We then reshuffle them as

$$\frac{d^2\hat{w}_R}{dz^2} - k_x^2\hat{w}_R - \frac{(\bar{u}(z)-c_R)\hat{w}_R - c_I\hat{w}_I}{(\bar{u}(z)-c_R)^2 + c_I^2}\bar{u}''(z) = 0$$
$$\frac{d^2\hat{w}_I}{dz^2} - k_x^2\hat{w}_I - \frac{c_I\hat{w}_R + (\bar{u}(z)-c_R)\hat{w}_I}{(\bar{u}(z)-c_R)^2 + c_I^2}\bar{u}''(z) = 0 \tag{6.14}$$

We then solve these equations numerically, using for instance a Newton-Raphson two-point boundary value relaxation method. To find the sinuous and varicose modes, we limit the domain to $z > 0$ and require that $d\hat{w}/dz = 0$ at $z = 0$ for the sinuous mode, and $\hat{w} = 0$ at $z = 0$ for the varicose mode. The figure below shows c_I as a function of k_x for the sinuous mode. We see that growing modes only exist for small enough k_x (that is, $k_x < 2$), and that there is a most rapidly growing mode whose wavenumber is approximately $k_x = 0.1$. For the varicose mode, the maximum wavenumber that is unstable is $k_x = 1$, and the growth rate of the varicose modes are always smaller than those of the sinuous modes (see Figure 6.3).

Interestingly, the marginal modes (that is, the modes for which c_I is identically zero) can be found analytically. It's easy to check that they have

$$k_x = 2\ ,\ c_R = \frac{2}{3}\ ,\ \hat{w} = \text{sech}^2(z) \text{ for the sinuous mode}$$
$$k_x = 1\ ,\ c_R = \frac{2}{3}\ ,\ \hat{w} = \text{sech}(z)\tanh(z) \text{ for the varicose mode} \tag{6.15}$$

The fact that c_R is equal to value of $\bar{u}(z)$ at the inflection point, for these marginal modes, is not a coincidence. It it the only real value of c_R for which a *non-singular* solution to Rayleigh's equation can exist.

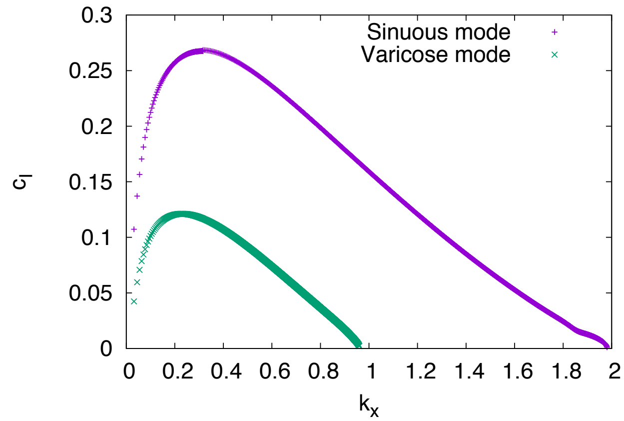

Figure 6.3: Imaginary part of c (which is proportional to the growth rate λ) for the sinuous and varicose modes.

Finally, note that in addition to the regular marginal and growing modes, there is also a continuum of singular modes whose eigenvalue c is real, and lies between 0 and 1. These can be found, as before, by seeking solutions on either sides of the singular point, and matching them to one another, and to the boundary conditions at infinity.

6.4 The viscous theory for shear instabilities

6.4.1 The background flow and the importance of viscosity

In the previous Section, we studied inviscid shear flows. These turn out to be somewhat peculiar in the sense that any profile $\bar{u}(z)$ could be used for the background shear. In reality, however, shear flows usually arise from a balance between forcing and viscous dissipation, and there is a single background solution for a given forcing and a given set of boundary conditions. Indeed, if we try to solve

$$\rho_m \left(\frac{\partial \boldsymbol{u}}{\partial t} + \boldsymbol{u} \cdot \nabla \boldsymbol{u} \right) = -\nabla p + \rho_m \nu \nabla^2 \boldsymbol{u} + F(z) \boldsymbol{e}_x \tag{6.16}$$

(where we have arbitrarily chosen to take the force as acting in the $x-$direction), then the only steady-state solution (assuming, say, periodic boundary conditions in x) is such that

$$\rho_m \nu \nabla^2 \bar{\boldsymbol{u}} + F(z) \boldsymbol{e}_x = 0 \tag{6.17}$$

or in other words,

$$\bar{\boldsymbol{u}} = \bar{u}(z) \boldsymbol{e}_x \tag{6.18}$$

where $\bar{u}(z)$ satisfies

$$\frac{d^2\bar{u}}{dz^2} = -\frac{F(z)}{\rho_m \nu} \tag{6.19}$$

The actual solution $\bar{u}(z)$ will then depend on what is assumed in terms of the boundary conditions in z. For a constant force F_0, for instance, with no-slip boundaries at $z = 0$ and $z = 1$ (so $\bar{u}(0) = \bar{u}(1) = 0$, we find that the solution is

$$\bar{u}(z) = -\frac{F_0}{\rho_m \nu}\frac{z(z-1)}{2} \tag{6.20}$$

or, in other words, a parabolic profile (called a *Poiseuille flow*). Other forces and other boundary conditions will similarly yield other background flow profiles $\bar{u}(z)$.

Since viscosity is key in selecting the background flow, it is often not a good idea to neglect it. For this reason, we now proceed to analyze the stability of shear flows in the presence of viscosity.

6.4.2 Linear stability

As in the case of inviscid shear flows, we now let $\boldsymbol{u} = \bar{\boldsymbol{u}} + \tilde{\boldsymbol{u}}$, and substitute this into the momentum equation. We get

$$\frac{\partial \tilde{\boldsymbol{u}}}{\partial t} + \bar{\boldsymbol{u}} \cdot \nabla \tilde{\boldsymbol{u}} + \tilde{\boldsymbol{u}} \cdot \nabla \bar{\boldsymbol{u}} = -\frac{1}{\rho_m}\nabla \tilde{p} + \nu \nabla^2 \tilde{\boldsymbol{u}} \tag{6.21}$$

With the same steps as in the case of inviscid flows, we arrive at

$$(\lambda + ik_x\bar{u}(z))\left(\frac{d^2\hat{w}}{dz^2} - k_x^2\hat{w}\right) - ik_x\hat{w}\frac{d^2\bar{u}}{dz^2} = \nu\left(\frac{d^2}{dz^2} - k_x^2\right)\left(\frac{d^2\hat{w}}{dz^2} - k_x^2\hat{w}\right) \tag{6.22}$$

which can then be transformed into the *Orr-Sommerfeld* equation:

$$(\bar{u}(z) - c)D\hat{w} - \hat{w}\frac{d^2\bar{u}}{dz^2} = -i\frac{\nu}{k_x}D^2\hat{w} \tag{6.23}$$

using, as before $\lambda = -ik_x c$ and where the operator $D \equiv d^2/dz^2 - k_x^2$

By contrast with Rayleigh's equation, the Orr-Sommerfeld equation is always regular (for $\nu \neq 0$), since the coefficient in front of the highest derivative is never 0. It is therefore much easier to find solutions numerically. However, the equation itself is of higher order and very rarely has any analytical solution. Some theorems associated with properties of solutions of the Orr-Sommerfeld equation are discussed by Drazin & Reid in the textbook *Hydrodynamic Stability*. The most important set of results concerning the stability of viscous shear flows are summarized in Chapter 4 (where they use the notation $R \propto 1/\nu$ for the Reynolds number, and $\alpha = k_x$). We see that

- In general, viscosity has a tendency to stabilize shear flows for very large values of ν (small values of R). For instance, the range of unstable modes for the Bickley jet (e.g. case (d)) is null below a critical value of R, and then gradually increases to recover the inviscid range for large R.

- This last statement is in fact true of all cases: for $R \to \infty$, the inviscid limit is indeed recovered (so it is not a singular limit of the equations).
- Interestingly, however, we also find that linear shear flows (which are linearly stable for all wavenumbers in the inviscid limit), can be unstable for an intermediate range of values of the viscosity. This is a peculiar case where viscosity can have a destabilizing effect on a system.

6.4.3 Energy stability for viscous linear shear flows

To finish this section on the stability of unstratified shear flows, we now look again at the problem of energy stability, using the method discussed in the context of convection. Let's consider a domain of height L_z, and horizontal size L_x, and assume for the moment that there is a linear background shear flow $\bar{u}(z) = S\boldsymbol{e}_z$. We assume that all the perturbations to that background are periodic in L_x and L_z. We now look at the energetics of perturbations $\tilde{\boldsymbol{u}}$ around that state. The governing equations are :

$$\begin{aligned}
&\frac{\partial \tilde{u}}{\partial x} + \frac{\partial \tilde{w}}{\partial z} = 0 \\
&\frac{\partial \tilde{u}}{\partial t} + \tilde{\boldsymbol{u}} \cdot \nabla \tilde{u} + Sz\frac{\partial \tilde{u}}{\partial x} + S\tilde{w} = -\frac{1}{\rho_0}\frac{\partial \tilde{p}}{\partial x} + \nu\nabla^2\tilde{u} \\
&\frac{\partial \tilde{w}}{\partial t} + \tilde{\boldsymbol{u}} \cdot \nabla \tilde{w} + Sz\frac{\partial \tilde{w}}{\partial x} = -\frac{1}{\rho_0}\frac{\partial \tilde{p}}{\partial z} + \nu\nabla^2\tilde{w}
\end{aligned} \tag{6.24}$$

Non-dimensionalizing the distances with respect to the vertical size L_z of the domain, and the velocity in terms of SL_z, we get the non-dimensional equations

$$\begin{aligned}
&\frac{\partial u}{\partial x} + \frac{\partial w}{\partial z} = 0 \\
&\frac{\partial u}{\partial t} + \boldsymbol{u} \cdot \nabla u + z\frac{\partial u}{\partial x} + w = -\frac{\partial \tilde{p}}{\partial x} + \frac{1}{\mathrm{Re}}\nabla^2 u \\
&\frac{\partial w}{\partial t} + \boldsymbol{u} \cdot \nabla w + z\frac{\partial w}{\partial x} = -\frac{\partial \tilde{p}}{\partial z} + \frac{1}{\mathrm{Re}}\nabla^2 w
\end{aligned} \tag{6.25}$$

where everything is now implicitely non-dimensional variables and where

$$\mathrm{Re} = \frac{SL_z^2}{\nu} \tag{6.26}$$

is the Reynolds number of the flow. The Reynolds number is another very famous number in fluid dynamics that measures the ratio of the inertial terms ($\boldsymbol{u} \cdot \nabla \boldsymbol{u}$) to the viscous terms ($\nu\nabla^2\boldsymbol{u}$). The larger the Reynolds number is, the less important viscosity is. In the limit of very large Reynolds number, viscosity should be negligible.

Using the usual trick of dotting the momentum equation with $\boldsymbol{u}$, we get the very simple energy equation

$$\frac{\partial E}{\partial t} = -\langle uw \rangle - \frac{1}{\mathrm{Re}}\langle |\nabla \boldsymbol{u}|^2 \rangle \equiv \mathcal{H}(\boldsymbol{u}) \tag{6.27}$$

As in the case of convection, we then try to determine when energy stability occurs, ie. when $\mathcal{H}(\boldsymbol{u})$ is negative for all possible divergence-free velocity fields.

We first maximize $\mathcal{H}(\boldsymbol{u})$ under the constraints that $\nabla \cdot \boldsymbol{u} = 0$ and the dissipation functional $\mathcal{D} = D_0$. To do so, we create the functional

$$\mathcal{S} = -\langle uw \rangle + \Lambda_1 \langle \frac{1}{\mathrm{Re}} |\nabla \boldsymbol{u}|^2 - D_0 \rangle + \langle \Lambda_2(x,z) \nabla \cdot \boldsymbol{u} \rangle \tag{6.28}$$

with the two Lagrange multipliers Λ_1 and $\Lambda_2(x,z)$. This defines the Lagrangian

$$\mathcal{L} = -uw + \Lambda_1 (\frac{1}{\mathrm{Re}} |\nabla \boldsymbol{u}|^2 - D_0) + \Lambda_2(x,z) \nabla \cdot \boldsymbol{u} \tag{6.29}$$

The Euler-Lagrange equations for this maximization process are:

$$\begin{aligned} -w &= \frac{\partial \Lambda_2}{\partial x} + 2\frac{\Lambda_1}{\mathrm{Re}} \nabla^2 u \\ -u &= \frac{\partial \Lambda_2}{\partial z} + 2\frac{\Lambda_1}{\mathrm{Re}} \nabla^2 w \end{aligned} \tag{6.30}$$

together with the two constraints. Eliminating Λ_2 between the two equations, we get

$$\frac{\partial u}{\partial x} - \frac{\partial w}{\partial z} = 2\frac{\Lambda_1}{\mathrm{Re}} \nabla^2 \left(\frac{\partial u}{\partial z} - \frac{\partial w}{\partial x} \right) \tag{6.31}$$

Since we are working in 2D we can use a streamfunction such that $u = \partial\phi/\partial z$ and $w = -\partial\phi/\partial x$. The equation above becomes

$$2\frac{\partial^2 \phi}{\partial x \partial z} = 2\frac{\Lambda_1}{\mathrm{Re}} \nabla^4 \phi \tag{6.32}$$

Assuming solutions of the kind $\phi(x,z) \sim \exp(ik_x x + ik_z z)$, this yields

$$\Lambda_1 = -\mathrm{Re} \frac{k_x k_z}{(k_x^2 + k_z^2)^2} \tag{6.33}$$

Let's now go back to the original energy equation, and calculate its right-hand-side:

$$\begin{aligned} \frac{\partial E}{\partial t} &= -\langle uw \rangle - \frac{1}{\mathrm{Re}} \langle \left(\frac{\partial u}{\partial x}\right)^2 + \left(\frac{\partial u}{\partial z}\right)^2 + \left(\frac{\partial w}{\partial x}\right)^2 + \left(\frac{\partial w}{\partial z}\right)^2 \rangle \\ &= \langle \frac{\partial \phi}{\partial x} \frac{\partial \phi}{\partial z} \rangle - \frac{1}{\mathrm{Re}} \langle \left(\frac{\partial^2 \phi}{\partial x \partial z}\right)^2 + \left(\frac{\partial^2 \phi}{\partial z^2}\right)^2 + \left(\frac{\partial^2 \phi}{\partial x^2}\right)^2 + \left(\frac{\partial^2 \phi}{\partial z \partial x}\right)^2 \rangle \\ &= -k_x k_z \langle |\phi|^2 \rangle - \frac{(k_x^2 + k_z^2)^2}{\mathrm{Re}} \langle |\phi|^2 \rangle \\ &= -\frac{(k_x^2 + k_z^2)^2}{\mathrm{Re}} (1 - \Lambda_1) \langle |\phi|^2 \rangle \end{aligned} \tag{6.34}$$

This implies that for the system to be energy-stable ($dE/dt < 0$), we simply need $\Lambda_1 < 1$ where $k_x^2 + k_y^2$ is not allowed to be identically 0 (otherwise $dE/dt = 0$). Since we can rewrite Λ_1 as

$$\Lambda_1 = -\mathrm{Re} \frac{\cos\theta \sin\theta}{k^2} = -\frac{\mathrm{Re}}{2} \frac{\sin 2\theta}{k^2} \tag{6.35}$$

where $k^2 = k_x^2 + k_z^2$ and $\cos\theta = k_x/k$, then we see that Λ_1 is maximum for angles $\theta = -\pi/4$ and $\theta - 3\pi/4$, in which case $\sin(2\theta) = -1$, but continuously decreases with increasing k^2. Hence, the maximum value of Λ_1 is for $k_x = \pm k_z$, and for the smallest non-zero available value of k that lies at these angles. This implies

$$\max \Lambda_1 = \frac{\mathrm{Re}}{2} \max_{k_x = \pm k_y} \frac{1}{k_x^2 + k_z^2} = \frac{\mathrm{Re}}{4} \frac{1}{\min(k_x^2, k_z^2)} = \mathrm{Re} \max(\hat{L}_x^2, 1) \tag{6.36}$$

where $\hat{L}_x = L_x/L_z$ is the horizontal length of the domain in units of L_z. To get to the last expression we have used the fact that the minimum wavenumber in the z direction is 2π, while the minimum wavenumber in the x direction is $2\pi/\hat{L}_x$. So, finally, the condition $\Lambda_1 < 1$ for energy stability implies a condition on the Reynolds number :

$$\mathrm{Re} < \mathrm{Re_E} = \frac{16\pi^2}{\max(L_x^2/L_z^2, 1)} \tag{6.37}$$

This shows that large enough viscosity (low enough Reynolds number) can always stabilize a shear flow.

The implication of this result for a square periodic domain, for instance, is that the maximum Reynolds number for stability[1] of a linear shear flow is $\mathrm{Re}_E = 16\pi^2 \simeq 158$. For larger Reynolds numbers, we know that the flow is linearly stable, but well-chosen finite amplitude instabilities can destabilize it. The question of the *optimal* perturbations, i.e. for a given perturbation energy, what is the shape of the perturbation that is unstable for the lowest possible Reynolds number, is a subject of active research.

[1]This is another good way of testing the numerics of a doubly-periodic code : for any $\mathrm{Re} < \mathrm{Re}_E$ the total energy of any initial perturbation should decay.